JOURNAL OF GEOPHYSICAL RESEARCH, VOL. 91, NO. C2, PAGES 2574–2580, FEBRUARY 15, 1986

Tracing the Amazon Component of Surface Atlantic Water Using ^{228}Ra, Salinity and Silica

WILLARD S. MOORE

Department of Geology, University of South Carolina, Columbia

JORGE L. SARMIENTO AND R. M. KEY

Geophysical Fluid Dynamics Program and Department of Geology and Geophysics, Princeton University, New Jersey

High $^{228}Ra/^{226}Ra$ activity ratios characteristic of waters in the Amazon estuary provide a sensitive indicator of the presence of these waters in the Atlantic Ocean. A conservative mixing model utilizing the $^{228}Ra/^{226}Ra$ activity ratio (AR) tied to absolute measurements in the estuary allows us to estimate that 20–34% of the surface water east of the Antilles during June, 5–9% from the same area during December, and 15–20% of the eastern Caribbean surface water during December are derived from the Amazon estuary. Differences in ^{228}Ra input occur in response to variable stratification of water near the river mouth. During high discharge, intense vertical mixing enriches the water in the estuary in ^{228}Ra. A large fraction of this water moves to the north and east of the Antilles, where its relatively high $^{228}Ra/^{226}Ra$ AR distinguishes it over 1500 km from its source. During low discharge (northern hemisphere fall) a significant fraction of river water passes northwest of the zone of intense mixing into a vertically stratified region where ^{228}Ra gain is lower. This water is transported by the Guiana Current along the coast of South America and into the Caribbean.

1. INTRODUCTION

River water contains several tracers which enable oceanographers to identify its effect on the ocean. Near the point of intrusion a turbid plume provides strong visual evidence of the presence of river water. Further offshore negative salinity and positive silica anomalies are the most common indicators of river water in the ocean. In this paper we shall introduce a new tracer, the $^{228}Ra/^{226}Ra$ activity ratio, for identifying river water thousands of kilometers from its riverine source.

Ryther et al. [1967] noted that Amazon River water was entrained in the Guiana Current and carried to the north and east where its presence could be recognized by anomalous salinity and nutrient composition and phytoplanktonic organisms. The low salinity and high silica contents were the best indicators. *Metcalf* [1968] proposed that a major interruption of the Guiana Current in the vicinity of the Amazon mouth allowed low-salinity water derived from the Amazon to penetrate as much as 650 km into the Atlantic Ocean.

During the BOMEX expedition, *Landis* [1971] observed low-salinity water (33‰) at 17°N in late July 1969. The BOMEX station network was arranged so that salinity contours clearly indicated that the Amazon River was the source of the freshened water.

Steven and Brooks [1972] determined that at a station near Barbados, salinity and silica were inversely correlated at 5- and 25-m depths but not at greater depths. Their observations, which extended for almost two years, clearly showed that the low-salinity water passed the sampling station as distinct pulses. *Borstad* [1982] related salinity differences near Barbados to meanders of the Guiana Current and noted lowest salinities during July–August and highest salinities during December–January.

Froelich et al. [1978] identified low-salinity, high-silica water in the central Caribbean, which they attributed to the Amazon and Orinoco rivers. Highest salinities were measured during April–May and lowest salinities occurred during late October to early November, directly out of phase with the observations near Barbados. Through a three-point conservative mixing model they were able to determine that at least 60% of the freshwater in these seasonal signals originated in the rivers rather than as precipitation. If silica was nonconservative, the relative proportion of river water could be even greater.

Moore [1981] and *Elsinger and Moore* [1983] demonstrated that estuarine processes enrich ^{228}Ra in relation to ^{226}Ra in the water. In direct measurements of the Amazon estuary, *Key et al.* [1985] measured $^{228}Ra/^{226}Ra$ activity ratios of 3.2 extending from 12 to 30‰ salinity. At 36‰ the activity ratio decreased to 0.39. The $^{228}Ra/^{226}Ra$ activity ratio thus provides a sensitive indicator of the presence of Amazon River water in the ocean. Once the water leaves the nearshore zone, the ratio will only change by decay of ^{228}Ra ($t^{1/2} = 5.7$ yrs.) and mixing. The salinity signal can change by precipitation and evaporation, and the silica signal can change by biological uptake, but these processes have no effect on the $^{228}Ra/^{226}Ra$ activity ratio.

2. SAMPLING AND MEASUREMENT TECHNIQUES

The samples were collected during the North Atlantic Study (NAS) and Tropical Atlantic Study (TAS) of the Transient Tracers in the Ocean (TTO) project (Figure 1). Surface water was sampled by suspending a bag of MnO_2-coated fiber (Mn-fiber) [*Moore*, 1976] in the water while on station or passing a sample through a column of Mn fiber. This sample was used to determine the $^{228}Ra/^{226}Ra$ activity ratio. At some stations, 30-liter surface water samples were carefully passed through a small Mn-fiber column to quantitatively extract ^{226}Ra [*Moore et al.*, 1985].

The $^{228}Ra/^{226}Ra$ activity ratio was determined by extracting the Ra from the fiber, coprecipitating with $BaSO_4$, and measuring gamma rays from ^{228}Ra and ^{226}Ra daughters in a well-type intrinsic germanium detector or WeGe detector [*Moore*, 1984]. The detector was calibrated using the latest

Paper number 5C0824.
0148-0227/86/005C-0824$05.00

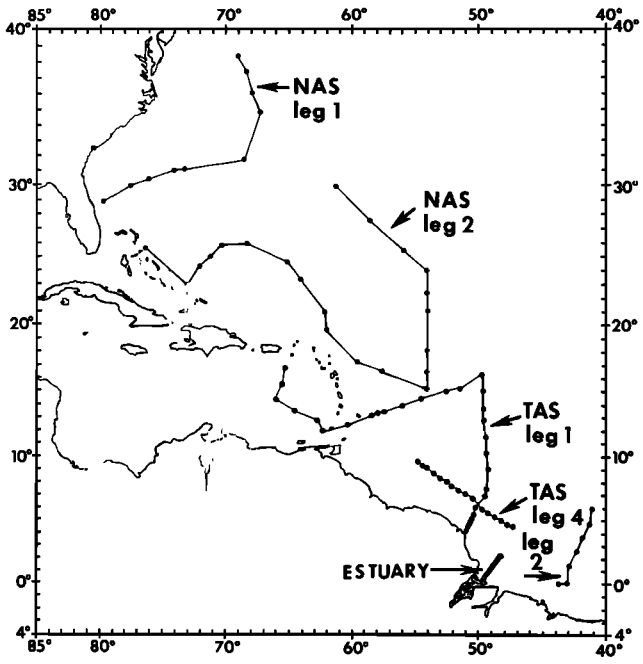

Fig. 1. Map of station locations identified by cruise names: NAS legs 1 & 2 (April-May 1981), TAS leg 1 & 2 (December 1982), TAS leg 4 (March 1983).

NBS standards. Radium 226 was determined using the procedures described by *Moore et al.* [1985].

These procedures allow a rapid assessment of the Ra isotope content of surface waters. No dedicated ship time and relatively little laboratory and counting time are required for these analyses.

3. Results

The full data for samples reported in this study are available from WSM.

The errors for the $^{228}Ra/^{226}Ra$ AR are generally $\leq \pm 5\%$ on the basis of a weighted means assessment of three gamma ray peaks for each isotope. These errors do not include uncertainties in the calibration of the detector or the relative uncertainties of the gamma ray intensity of each peak. Such uncertainties may add another 2 to 4% to the absolute uncertainty of these measurements, but because the samples were measured in standard geometry in a single detector, they do not affect the relative uncertainties.

Throughout this discussion we refer to changes in ^{228}Ra as changes in the $^{228}Ra/^{226}Ra$ activity ratio. This is because we have a great deal more data on the activity ratios than on the absolute ^{226}Ra activities that we use to compute absolute ^{228}Ra. We may sacrifice some information by only using activity ratios, but this does not seem to be a major problem. We do have excellent control for ^{226}Ra in the Amazon estuary and for the TAS leg 4 samples (Figure 2). The estuary data fall very close to a simple mixing line of the freshwater end-member and the maximum activity encountered in the estuary (21.5‰ salinity), and the leg 4 samples fall within a triangle formed by this line and another mixing line connecting the estuary maximum with the offshore end-member. Note that for offshore samples the ^{228}Ra varies between 3 and 55 dpm/100 L, whereas the ^{226}Ra only varies between 8 and 21 dpm/100 L. So although a doubling of the $^{228}Ra/^{226}Ra$ AR in offshore waters corresponds to more than a factor of 2 increase in ^{228}Ra activity, the trend in each isotope is similar. Thus, little information is lost using the activity ratio as compared to the absolute ^{228}Ra activity.

During legs 1 and 2 of NAS (April–May 1981) (Figure 3), high $^{228}Ra/^{226}Ra$ ARs are observed in the 5 southernmost stations (16°–20°N, 55°–60°W). The rest of the legs 1 & 2 NAS samples show a rather consistent AR of 0.4 ± 0.1.

During leg 1 of TAS (December 1982) (Figure 3), high ARs (>0.8) were measured throughout the eastern Caribbean Sea and immediately off the coast of South America; however, only moderate values (0.4–0.5) were encountered at the closest approach to the NAS leg 2 track where high values had been measured in May. Two high values (0.68, 0.74) were measured along this track at ~10°N, 50°W (Stations 22 and 23) and were clearly separated from the high nearshore values by waters of lower AR (0.2). At the end of leg 1 the Knorr entered the Amazon estuary, and it was here that the very highest (>3) ARs were measured. We refer to this segment of leg 1 as the estuary to distinguish the samples collected from the remainder of TAS leg 1 samples. A full description of the estuary transect has been published by *Key et al.* [1985]. TAS leg 2 (perpendicular to the South American coast south of the Amazon) encountered water with a consistently low AR of 0.20 ± 0.02.

TAS leg 4 (February 1983) (Figure 3) was parallel to the coast of South America, and the water sampled had a range of ARs equilvalent to all of the other surface NAS and TAS samples. Again, the patchiness of the signal was very evident. Samples having ARs of 0.15 and 0.53 were sandwiched between samples having ARs of 1.83 and 3.24.

4. Silica-Salinity Relationships

Significant differences exist in the relation of silica to salinity. For inshore samples, two distinct trends are evident. Sam-

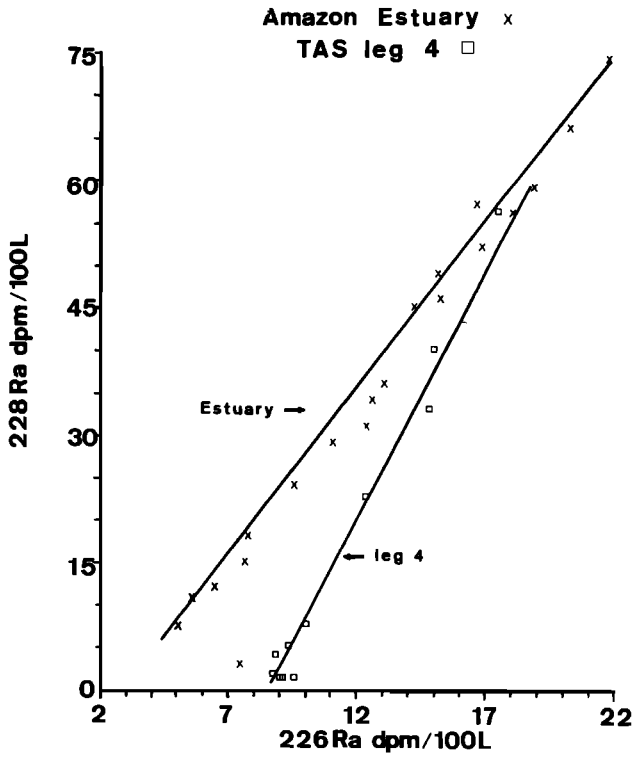

Fig. 2. Radium 228: radium 226 relationship in the Amazon estuary and TAS leg 4 samples collected offshore of the estuary.

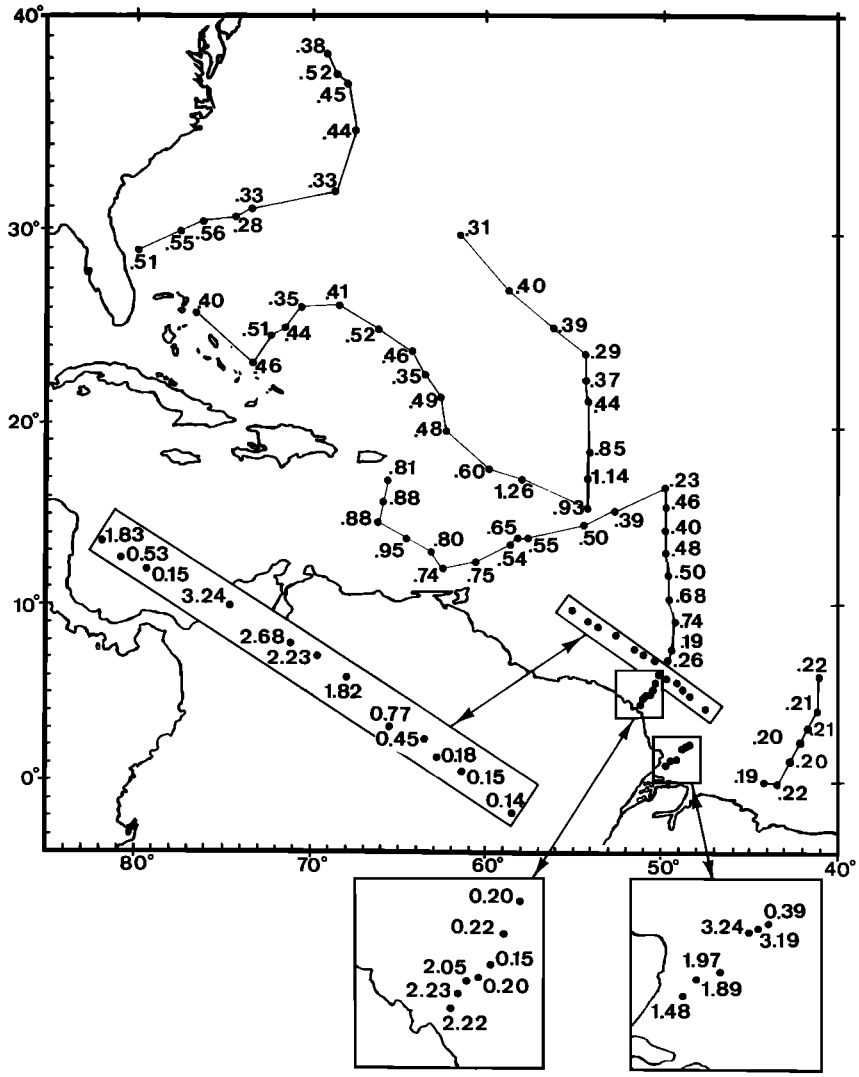

Fig. 3. Data for $^{228}Ra/^{226}Ra$ activity ratios in surface waters. See Figure 1 for cruise identification and date.

ples collected in the Amazon estuary from 0–21.5‰ salinity and reported by *Key et al.* [1985] and the two most inshore samples collected on TAS leg 1 north of the Amazon estuary have a silica-salinity (Si-Sal) slope of -3.7 μm/gm. Samples collected in the Amazon estuary at salinities above 22‰, samples from TAS leg 1 above 28‰, and all samples from TAS leg 4 have a Si-Sal slope of only -1.3 μm/gm (Figure 4). The differences encountered in the Amazon estuary were explained by *Key et al.* [1985] as originating from different source regions with the high-salinity, relatively low silica samples being derived from the Para distributary of the Amazon. However, *Key et al.* [1985] point out that higher biological productivity above 21‰ salinity could be responsible for the differences observed.

Further offshore, more subtle Si-Sal differences are observed. TAS leg 1 samples in the 34-37‰ salinity range have a Si-Sal slope of -1.7 μm/gm (Figure 5). This slope is almost identical to the slope of the TAS leg 1 samples above 28‰ and to the slope of -1.6 μm/gm measured by *Froelich et al.* [1978] in the Caribbean Sea. NAS leg 2 samples have a lower gradient of -0.55 μm/gm, which is similar to a gradient of -0.59 μm/gm reported by *Steven and Brooks* [1972] for samples collected near Barbados. Thus it appears that waters entering the Caribbean have different Si-Sal relationships from low-salinity waters that move to the east of the Antilles.

On the basis of these data alone it is difficult to determine the relative effects of biological activity, freshwater precipitation, and different source regions in determining the Si-Sal relationship.

5. $^{228}Ra/^{226}Ra$ AR-Salinity Relationships

A plot of the $^{228}Ra/^{226}Ra$ AR versus salinity (AR-Sal) in the 13–37‰ salinity range (Figure 6) reveals that the estuary samples have an AR which is practically constant at 3.20 ± 0.15. The low-salinity (20-28‰) TAS leg 1 samples have considerably lower ARs of 2.17 ± 0.10. One of the TAS leg 4 samples has an AR of 3.24, the same as the estuary samples, but another has an AR of 2.23 at a salinity of 27.4‰, the same as TAS leg 1 samples of similar salinity. A third low-salinity TAS leg 4 sample has an AR falling between these two types.

In the Amazon estuary, excess ^{226}Ra (the amount above a conservative mixing of river and sea waters) is supplied primarily by desorption from river-borne particles [*Key et al.*, 1985]. Radium 228 is supplied by this source and by release from estuarine sediments. Little ^{226}Ra is derived from estuarine sediments because its half life (which is proportional to the

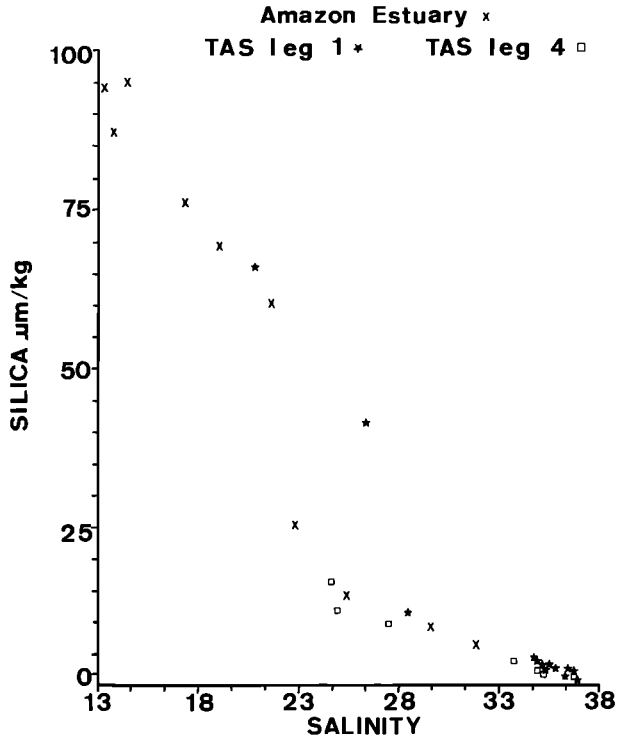

Fig. 4. Silica-salinity relationships in the 13–37‰ salinity range.

time required for ^{230}Th in the sediments to generate new ^{226}Ra activity) is 1600 years. New activity of ^{228}Ra is generated in proportion to its 5.7-year half life. Thus sediments that are in active contact with estuarine waters lose ^{226}Ra activity once but lose ^{228}Ra activity many times before they are buried by new sediments. The flux of ^{228}Ra from the estuarine sediments elevates the AR to a level determined by the residence time of the water in contact with the sediments and the ^{228}Ra/^{226}Ra AR supplied by the sediments (11.2 by Key et al.'s estimate). Apparently, the low-salinity waters sampled on TAS leg 1 northwest of the estuary had not stayed in contact with the estuary sediments long enough to achieve the high AR characteristic of the estuarine samples. The TAS leg 4 samples apparently represent mixtures of waters having high and low contact times with estuarine sediments.

Gibbs [1970] reported that during high-discharge conditions, no salt wedge entered the Amazon estuary, and turbulent mixing extended throughout the water column up to 80 km offshore. During low discharge he noted that the zone of vertical mixing extended only 60 km offshore.

Edmond et al. [1981] found that shoal areas adjacent to the Amazon mouth were areas of intense vertical mixing and upwelling where the halostratification was broken down and nutrient-enriched waters and resuspended detrital sediments were introduced to the surface layer. Northwest of the mouth the water column was highly stratified with low-salinity surface waters out of contact with the bottom [*Edmond et al.*, 1981; *DeMaster et al.*, 1983].

Vertical mixing and resuspension of bottom sediments should increase the ^{228}Ra/^{226}Ra AR in unstratified waters near the Amazon mouth. However, Amazon water that passes to the stratified region north of the mouth with limited time in the zone of intense mixing should have less ^{228}Ra input and a lower AR. This is what we observe.

In the salinity range 34–37‰ there is a distinct difference in the AR-Sal relationship for NAS leg 2 and TAS leg 1 samples (Figure 7). Most of the TAS leg 1 samples have significantly lower ARs than NAS leg 2 samples of similar salinity. These differences may also be explained by postulating that most of the TAS leg 1 samples represent an estuarine component that left the estuary before receiving maximum ^{228}Ra input.

6. Unmixing the Amazon Estuary Component

If we assume conservation of salt and radium, we can write equations which may be solved for various combinations of radium isotopes and salinity to yield an estimate of the contribution of the Amazon estuary to Atlantic and Caribbean surface waters. We expect these processes to operate on a time scale of months, so we ignore ^{228}Ra decay.

1. Water conservation $V_{obs} = V_{oc} + V_{es} - (E - P)$ defined;

obs	observed value
oc	ocean end-member
es	estuary end-member
E	evaporation
P	precipitation
f	fraction

$$f_{oc} = \frac{V_{oc}}{[V_{oc} + V_{es} - (E - P)]}$$

$$f_{es} = \frac{V_{es}}{[V_{oc} + V_{es} - (E - P)]}$$

$$f_{E-P} = \frac{-(E - P)}{[V_{oc} + V_{es} - (E - P)]}$$

Therefore,

$$f_{oc} + f_{es} + f_{E-P} = 1 \quad (1)$$

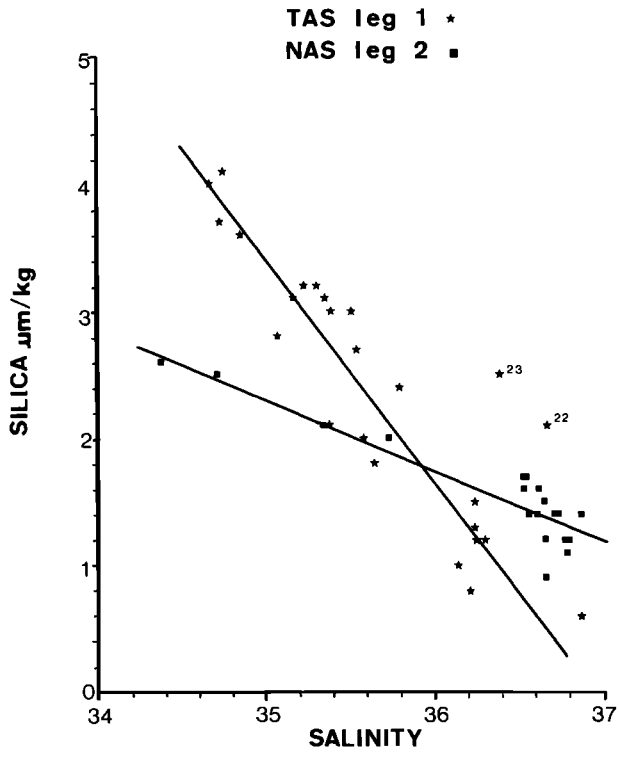

Fig. 5. Silica-salinity relationships in the 34–37‰ salinity range. For TAS leg 1 samples, $r^2 = 0.90$, and the slope of the line is -1.70 µm/gm. Samples 22 and 23 are omitted from this correlation. For NAS leg 2 samples, $r^2 = 0.85$, and the slope is -0.55 µm/gm.

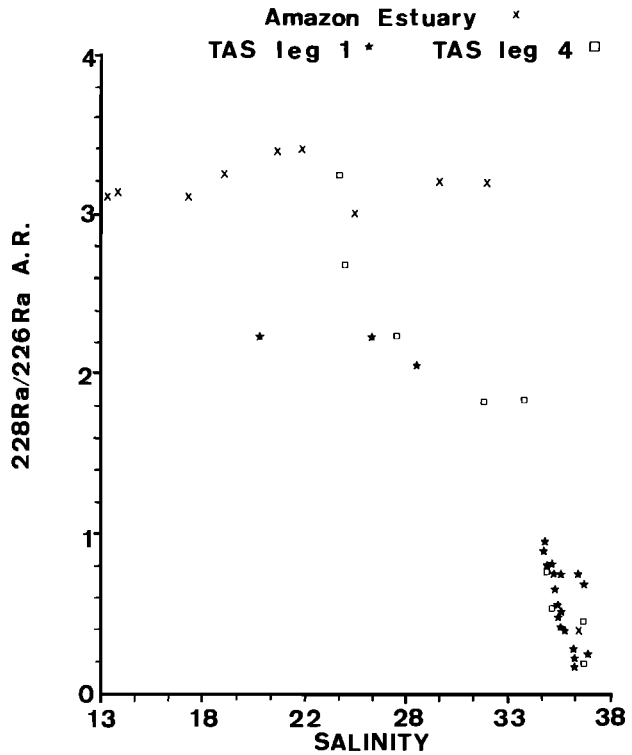

Fig. 6. Radium 228/radium 226 AR–salinity relationships in the 13–37‰ salinity range.

2. Salt conservation (The effect of evaporation and precipitation are implicit in the f_{oc} and f_{es} terms.):

$$S_{obs}V_{obs} = S_{oc}V_{oc} + S_{es}V_{es}$$
$$S_{obs} = S_{oc}f_{oc} + S_{es}f_{es} \quad (2)$$

3. Radium conservation, ignoring decay:

$$AR_{obs} = \frac{A\,^{228}Ra_{obs}}{A\,^{226}Ra_{obs}} = \frac{^{228}Ra_{oc}f_{oc} + {}^{228}Ra_{es}f_{es}}{^{226}Ra_{oc}f_{oc} + {}^{226}Ra_{es}f_{es}} \quad (3)$$

The unknowns are f_{oc}, f_{es}, and f_{E-P}

We obtain from (2) and (3)

$$f_{es} = \frac{\frac{S_{obs}}{S_{oc}}[AR_{obs}\,{}^{226}Ra_{oc} - {}^{228}Ra_{oc}]}{AR_{obs}\,{}^{226}Ra_{es} - {}^{228}Ra_{es} - \frac{S_{es}}{S_{oc}}}$$

And from (2)

$$f_{oc} = \frac{S_{obs} - S_{es}f_{es}}{S_{oc}}$$

And from (1)

$$f_{E-P} = 1 - f_{oc} - f_{es}$$

Thus by determining end-member activities of ^{228}Ra and ^{226}Ra in the estuary and ocean and the salinities of these end-members, the system is uniquely defined. Figure 8 is a map of the estuarine component in the Atlantic and Caribbean using the following end-members:

$$S_{es} = 31.8‰$$
$$^{228}Ra_{es} = 45 \pm 2 \text{ dpm/100 L}$$
$$^{226}Ra_{es} = 14.2 \pm 0.3 \text{ dpm/100 L}$$
$$S_{oc} = 36.2‰$$
$$^{228}Ra_{oc} = 1.2 \pm 0.2 \text{ dpm/100 L}$$
$$^{226}Ra_{oc} = 8.90 \pm 0.02 \text{ dpm/100 L}$$

We also computed the estuarine fractions using an estuarine end-member of 21.5‰, $^{228}Ra = 74 \pm 2$ dpm/100 L, and $^{226}Ra = 21.7 \pm 0.4$ dpm/100 L. This reduced the computed Amazon components in the ocean by about 30%.

We present this model as an illustration of how ^{228}Ra may be used to trace the estuary component. Before a comprehensive accounting of the Amazon contribution to the surface Atlantic may be completed, several factors must be understood better. For example, do the end-member compositions vary with time? Our own measurements suggest that during low-flow conditions, water with a lower AR and relatively low salinity moves to the north of the estuary. If such an end-member were used in the model, the Caribbean surface waters with which this end-member appears to mix would have a significantly higher component of Amazon estuary water. The role of the Orinoco River which may contribute to the Caribbean signal has not been evaluated. Other factors that would have to be considered in a comprehensive model are additional inputs and sinks of radium such as diffusion from nearshore sediments away from the estuary (although this is probably minimal for stratified waters) and radioactive decay. Biological utilization of radium should not affect the model

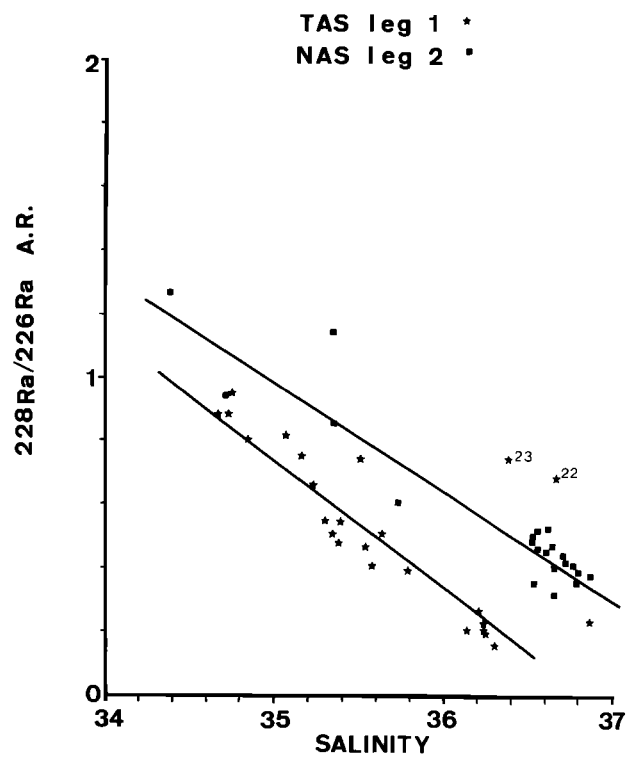

Fig. 7. Radium 228/radium 226 AR–salinity relationships in the 34–37‰ salinity range. For TAS leg 1 samples, $r^2 = 0.87$ with a slope of -0.40 per ‰. Samples 22 and 23 are omitted from this correlation. For NAS leg 2 samples, $r^2 = 0.89$ with a slope of -0.34 per ‰.

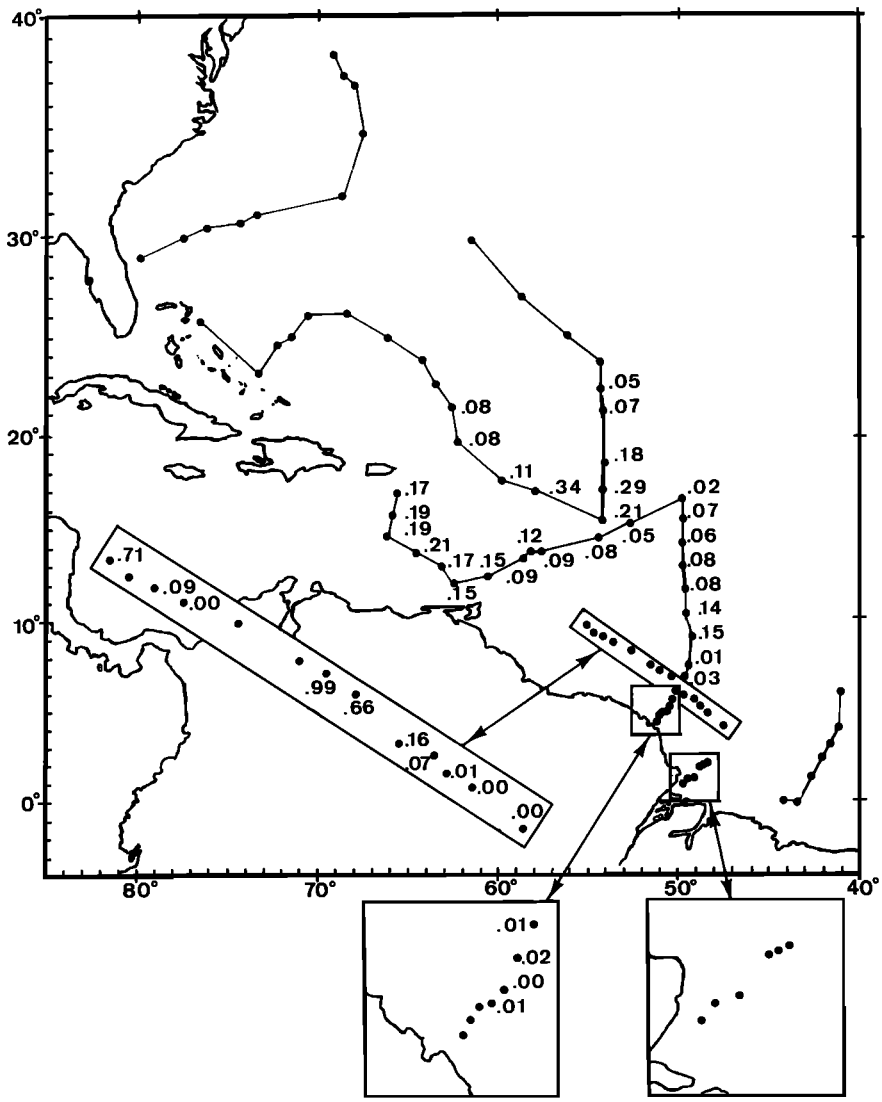

Fig. 8. Map of the estuarine component f_{es} in the Atlantic and Caribbean surface waters using the model and end-members discussed in the text. Note that these data are not synoptic (see Figure 1).

because the two radium isotopes should be utilized in the same AR as they occur; however, biological removal in the estuary could change the end-member concentrations.

7. Temporal Variability of the Signals

Borstad [1982], in a summary of his measurements and those of earlier workers near Barbados, noted maximum salinities during winter (December–January) and minimum salinities during summer (July–August). *Ryther et al.* [1967] found that freshwater lenses were restricted to an area fairly close to the Brazil coast during October–December, but during May–June, freshwater lenses occurred much further north.

In contrast to the observations east of the Antilles, *Froelich et al.* [1978] measured maximum freshening in the Caribbean during October–November and highest salinities during April–May.

Our sampling was fortuitously arranged so that we sampled the area NE of Barbados during May (NAS leg 2) and entered the Caribbean during December (TAS leg 1). Thus we sampled each area during the time maximum freshening had historically been recorded. We also repeated the sampling of the region NE of Barbados during December.

Our studies support the observations that Amazon River injections supply fresh water to the Caribbean during the winter when river discharge is a minimum and to the area NE of Barbados in the spring and early summer when the river discharge is maximum.

Recent studies of ship drift observations [*Richardson and McKee*, 1985] and high-resolution equatorial models [*Philander and Pacanowski*, 1984] show that the near coastal currents change quite dramatically with season in association with the annual cycle of the North Equatorial Countercurrent. The North Equatorial Countercurrent, which occupies the region between 5°N and 10°N, is at its maximum in the Northern Hemisphere summer and essentially nonexistent in winter [*Boisvert*, 1967; *Garzoli and Katz*, 1983; *Philander and Pacanowski*, 1984; *Richardson and McKee*, 1985] owing to changes in the wind forcing [*Garzoli and Katz*, 1983]. The Guiana Current contributes to the North Equatorial Countercurrent during the summertime, with a portion of it turning away from the coast toward the east. The freshwater lens referred to as the Amazon Anticyclone by *Cochrane et al.* [1979] forms

where the Guiana Current turns offshore during the summer and may be related to the presence of eddies in this region [*Bruce*, 1984]. We believe that the variability observed at Barbados is also related to the changes in the coastal flow, with the lower summertime salinities corresponding to the time that the coastal currents develop a stronger eastward component.

Our data indicate that the mixing pathways carrying water to each region are different. In high-discharge conditions during winter when the North Equatorial Countercurrent is very weak, water passes through the estuary where there is strong vertical mixing, loss of Si, and maximum gain of ^{228}Ra. Water following this path enters the Atlantic and flows to the north and east of the Antilles. The alternate pathway is most pronounced during the summer. Water of <22‰ salinity is carried into a vertically stratified region to the north of the estuary where contact with bottom sediments and vertical mixing are inhibited. This relatively high silica, low-^{228}Ra water is carried by the Guiana Current along the South American coast and into the Caribbean.

As usual, more data would be useful in confirming these observations. Nevertheless, the ^{228}Ra data provide a clear signature of the source of the freshened waters consistent with historical observations. During December, 15–20% of the Caribbean surface water was derived from the Amazon estuary, but only 5–9% of the water near Barbados was from this source. During May, 20–34% of the surface water near Barbados came from the Amazon estuary. Although the data are patchy, the signal is quite evident.

8. CONCLUSIONS

The ^{228}Ra/^{226}Ra activity ratio provides a sensitive indicator of the presence of river water in the ocean which may be identified thousands of kilometers from the riverine source. Using a conservative mixing model we can estimate the proportion of Atlantic and Caribbean surface waters originating in the Amazon estuary. The transport of these waters responds to the seasonal wind and current regimes.

1. During periods of high Amazon discharge (northern hemisphere summer) a large fraction of the river water passes through a zone of intense vertical mixing near the river mouth. Maximum ^{228}Ra input and silica removal occur before this water is transported into the Atlantic, where its northward flow causes freshened conditions in the surface waters east of the Antilles.

2. During periods of low Amazon discharge (northern hemisphere winter), a large fraction of the river water passes to the northwest of the zone of intense mixing into vertically stratified waters. The input of ^{228}Ra to these waters is less than for waters passing through the zone of intense vertical mixing. These waters, which are relatively lower in ^{228}Ra/^{226}Ra AR, are carried by the Guiana Current into the Caribbean.

Acknowledgments. We thank R. Stallard, F. Bryan, and the Physical and Chemical Oceanographic Data Facility for their assistance in collecting the samples and hydrographic data. Larry Triboletti, Roger Mahannah, Rhonda Levy, and JoLynn Butts assisted in the analyses of the samples and data. Comments by David DeMaster and Rana Fine strengthened the manuscript. Figures were drafted by G. Collins, and the manuscript was typed by Joyce Goodwin. Financial support was provided by NSF grants OCE8216611 and OCE8415964 to WSM and OCE-8117846 and OCE-83-15931 to JLS.

REFERENCES

Boisvert, W. E., Major currents in the north and south Atlantic Oceans between 64°N and 60°S, *Tech. Report*, Naval Oceanographic Office, NSTL Station, Miss., 92 pp., 1967.

Borstad, G. A., The influence of the meandering Guiana Current and Amazon River discharge on surface salinity near Barbados, *J. Mar. Res.*, *40*, 421–434, 1982.

Bruce, J. G., Comparison of eddies off the north Brazilian and Somali coasts, *J. Phys. Oceanogr.*, *14*, 825–832, 1984.

Cochrane, J. D., F. J. Kelly, Jr., and C. R. Olling, Subthermocline countercurrents in the western equatorial Atlantic Ocean, *J. Phys. Oceanogr.*, *9*, 724–738, 1979.

DeMaster, D. J., G. B. Knapp, and C. A. Nittrouer, Biological uptake and accumulation of silica on the Amazon continental shelf, *Geochem. et Cosmochem. Acta*, *47*, 1713–1723, 1983.

Edmond, J. M., E. A. Boyle, B. Grant, and R. F. Stallard, The chemical mass balance in the Amazon Plume, I, The nutrients, *Deep Sea Res.*, *28A*, 1339–1374, 1981.

Elsinger, R. J., and W. S. Moore, Ra-224, Ra-228 and Ra-226 sources in Winyah Bay and Delaware Bay, *Earth Planet. Sci. Lett.*, *64*, 430–436, 1983.

Froelich, P. N., Jr., D. K. Atwood, and G. S. Giese, Influence of Amazon River discharge on surface salinity and dissolved silicate concentrations in the Caribbean Sea, *Deep Sea Res.*, *25*, 735–744, 1978.

Garzoli, S. L., and E. J. Katz, The forced annual reversal of the Atlantic North Equatorial Countercurrent, *J. Phys. Oceanogr.*, *13*, 2082–2090, 1983.

Gibbs, R. J., Circulation in the Amazon River estuary and adjacent Atlantic Ocean, *J. Mar. Res.*, *28*, 113–123, 1970.

Key, R. M., R. Stallard, W. S. Moore, and J. L. Sarmiento, Distribution and flux of ^{226}Ra and ^{228}Ra in the Amazon River estuary, *J. Geophys. Res.*, *90*, 6995–7004, 1985.

Landis, R. C., Early BOMEX results of sea surface salinity and Amazon River water, *J. Phys. Oceanogr.*, *1*, 278–281, 1971.

Metcalf, W. G., Shallow currents along the northeastern coast of South America, *J. Mar. Res.*, *26*, 232–243, 1968.

Moore, W. S., Sampling ^{228}Ra in the deep ocean, *Deep-Sea Res.*, *23*, 647–651, 1976.

Moore, W. S., Radium isotopes in the Chesapeake Bay, Estuarine, *Coastal Shelf Sci.*, *12*, 713–723, 1981.

Moore, W. S., Radium isotope measurements using germanium detectors, *Nucl. Instrum. Meth. Phys. Res.*, *223*, 407–411, 1984.

Moore, W. S., R. M. Key, and J. L. Sarmiento, Techniques for precise mapping of ^{226}Ra and ^{228}Ra in the ocean, *J. Geophys. Res.*, *90*, 6983–6994, 1985.

Philander, S. G. H., and R. C. Pacanowski, Simulation of the seasonal cycle in the tropical Atlantic Ocean, *Geophys. Res. Lett.*, *11*, 802–804, 1984.

Richardson, P. L., and T. K. McKee, Average seasonal variations of the Atlantic Equatorial Currents from historical ship drifts. *J. Mar. Res.*, in press, 1985.

Ryther, J. H., D. W. Menze, and N. Corwin, Influence of the Amazon River outflow on the ecology of the western tropical Atlantic, I, Hydrography and nutrient chemistry, *J. Mar. Res.*, *25*, 69–83, 1967.

Steven, D. M., and A. L. Brooks, Identification of Amazon River water at Barbados, W. Indies by salinity and silicate measurements, *Mar. Biol.*, *14*, 345–348, 1972.

R. M. Key and J. L. Sarmiento, Geophysical Fluid Dynamics Program, Princeton University, P. O. Box 308, Princeton, NJ 08542.

W. S. Moore, Department of Geology, University of South Carolina, Columbia, SC 29208.

(Received May 24, 1985;
accepted July 10, 1985.)